SSRG International Journal of Electrical and Electronics Engineering
ISSN: 2348-8379/ https://doi.org/10.14445/23488379/IJEEE-V11I12P109

Volume 11 Issue 12, 100-107, December 2024

Original Article

Lumped Disturbance Estimation-Based Dynamic Surface Control for 8/6-Type Switching Reluctance Machines

Thuy Vo Thi Cam[1,3], Dzung Manh Do[2], Khoat Nguyen Duc[3], Phan Xuan Minh[4]

[1]*Faculty of Electrical Engineering, Hanoi University of Industry, Bac Tu Liem District, Hanoi, Vietnam.*
[2]*Faculty of Mechanical Engineering and Mechatronics, Phenikaa University, Yen Nghia, Ha Dong, Hanoi 12116, Vietnam*
[3]*Faculty of Mechanics and Electricity, University of Mining and Geology, Bac Tu Liem District, Ha Noi, Vietnam*
[4]*Faculty of Applied Sciences, International School, Vietnam National University, Cau Giay District, Hanoi 100000, Vietnam*

[2]*Corresponding Author: dung.domanh@phenikaa-uni.edu.vn*

Received: 06 October 2024 Revised: 07 November 2024 Accepted: 05 December 2024 Published: 31 December 2024

Abstract *- This paper concentrates on two problems in controlling the 8/6-type Switching Reluctance Motors (8/6-type SRMs or SRMs for short) in the presence of unknown external disturbances and uncertain factors. The first is studying the stabilization problem for SRMs' rotational speed, and the other is the disturbance rejection. The stabilization issue for SRMs' velocity is known as steering the rotational speed to be stable at the desired value, which is chosen arbitrarily, while disturbance rejection's primary mission is to eliminate external disturbances that harm SRMs' control performance. The first problem is handled by Dynamic Surface Control (DSC), in which the Low-Pass Filter (LPF) is integrated into the control scheme to perform the derivative operation of virtual control signals. This feature helps to reduce the computational burden and avoid the undesired phenomenon called "explosion of terms". The external disturbances presenting during the SRMs' operation are compensated via an online training Radial Basis Function (RBF) neural network. The control cooperation regime between the DSC and the proposed neural network for uncertain SRMs lifts the control performance compared to the traditional DSC. The effectiveness of contributions and control schemes is demonstrated through impressive mathematical proofs and numerical simulation platforms.*

Keywords *- Switching Reluctance Motor, Dynamic Surface Control, Disturbance compensation, Neural network*

1. Introduction

The 8/6-type Switched Reluctance Motors (8/6-type SRMs or SRMs for short) are a type of motor that has received much attention in recent years because of its outstanding advantages such as low manufacturing cost, long life and being less influenced by environmental temperature. However, SRMs still have some disadvantages during operation, such as large torque ripples, loud vibrations, and difficulty controlling them. These disadvantages are the main motivation for us to study scientific works related to the subject of SRMs. Research on SRMs in recent years has mainly focused on improving the quality of SRMs through two approaches: modelling SRMs with higher accuracy [1-3] and proposing new control strategies for SRMs' torque and rotational speed [5, 6, 8-12]. Regarding the first topic, papers [2, 3] have fully and detailedly studied the structure of SRMs, each part's functions, and the iron core's magnetization properties. Following this approach, Rigatos and his colleagues proposed a new engine model of SRMs in their work [1] in which the switching processes of semi-conductors, leading to the continuous high-frequency harmonics, have been integrated into the electro-mechanical model of the SRMs. Although the switching process of each phase in [1] is assumed to be instantaneous, meaning when one switch opens, another switch immediately closes, this is also a significant contribution in the context of previous works, where the authors only consider the separate activities of each phase [2], [3] and evaluating SRMs' operation during one phase open. Comprehensively considering the instantaneous switching process of 4 phases ensured the phase-mismatch phenomenon cannot happen, recognized as a harmful phenomenon in controlling motors and power electronic systems [3], may result in the loss of synchronization or damage in SRMs motor. The work of Rigatos [1] inspires this paper to construct a new strategy to address the uncertain dynamics presented in SRMs' operation, such as external disturbance. Regarding the second direction, direction mainly includes two main research topics, which are focusing on controlling the SRMs' rotational speed at desired values [5, 6, 8–11], so-called control problem stability, and improving output torque quality [14–16]. The control algorithms researched and applied to SRMs are relatively diverse, from linearised control techniques [1] to methods of the nonlinear class [8, 9] or persistent nonlinearity [5, 6]. The prominent methods among them are sliding control

techniques [5, 6, 11, 12] and Backstepping control techniques [9, 8–10]. Both sliding control and backstepping control require mathematical models of SRMs with full mathematical equations representing the electrical-electromagnetic connection to design the controller successfully. However, due to the characteristics of switched reluctance motors, each method has its own advantages and disadvantages. The sliding controller has been studied in works [5, 6, 11, 12]. In work [5], the sliding surface used has a linear constant coefficient form and is combined with a 2-position relay stage to implement the speed control law. With the goal of completely eliminating overregulation while maintaining the control structure's sustainability, in [6], the author proposed using the second-order sliding technique (SO-SMC) applied to SRMs. In particular, the control signal is also separated into two components (quasi-model and sliding), and the sliding surface used has a similar linear shape [5].

Although works on sliding control [5, 6, 11, 12] have achieved improvements and have certain advantages, no work has been able to avoid (or chattering at both engine speed and output torque. When considering the motor structure, it is shown that during the process of sequential switching between phases, due to the approximate assumption that the phases open and close instantaneously, the power conversion phase circuit itself is inherently generated. Immensely strong pulsing effect on output torque. If the pulsation phenomenon caused by the chattering effect of sliding control is added, the vibration amplitude and frequency will be extremely large [5, 6]. This causes load instability, imbalance in mechanical properties and an unpleasant noise when the engine operates.

Based on the inheritance of the nonlinear mathematical model of SRMs from the work [1], the Backstepping control method has been proposed to stabilize the speed for SRMs [7], [8– 10]. With the particularity of the method being applied specifically to the class of strictly feedback nonlinear systems, the classic Backstepping algorithm in [7] has been applied to SRMs by synthesizing the electrodynamic model for phase currents with the rotor's mechanical rotation. Therefore, the results in [7] show that the motor speed is stable and smooth at the set value. The Backstepping technique is also used in [5] in combination with a disturbance observer to give the control scheme adaptability in addition to stability.

Applying the Backstepping control algorithm can generally eliminate high-frequency vibration in both the control signal and the output circuit torque. But this comes at the expense of the sustainability of the closed system. Regardless of whether a disturbance hits the system, the quality of speed stability control given by Backstepping will be significantly affected. This has been proven in the work [7]. In addition, it must be added that the phenomenon of pulsation due to high-order harmonics of the switching process cannot be eliminated with the Backstepping technique. For the switching process, high-frequency harmonics generated by the continuous transition of the four phases reduce the control quality, leading to instability of the closed-loop system in bad cases. Therefore, this paper proposes a new solution to eliminate this undesired phenomenon: integrating a low-pass filter into the Backstepping controller. A Low-Pass Filter (LPF) not only has the effect of removing high frequencies but also has the ability to avoid the "explosion of terms" in calculating the derivative of the virtual control signal at intermediate steps, which significantly simplifies the virtual signal. A backstepping controller combined with a low-pass filter is called a Dynamic Surface Control (DSC).

The DSC method was used to design a controller for nonlinear SRMs affected by disturbances and has proven its suitability. The stability of the closed-loop control system is shown in the process of synthesizing the control law based on the Lyapunov criteria. This method is dominant when the system is affected by high-frequency disturbances, so it is suitable for SMR because SMR works in switching mode when operating. That is the primary contribution of this paper. To mitigate the impact of external disturbances, such as random white noise, that can adversely affect system performance, this paper proposes the application of the Radial Basis Function (RBF) as a tool to estimate and counteract unwanted environmental noise.

The RBF is widely recognized for its effectiveness in approximating uncertain or unknown functions, making it a suitable choice for addressing the variability in environmental conditions that might otherwise degrade the performance of control systems (ref). Integrating the RBF into the control scheme of Switched Reluctance Motors (SRM) represents a novel approach that significantly enhances the adaptability of the closed-loop SRM system, allowing it to maintain optimal performance despite the presence of disturbances. Moreover, the training function of the RBF network is derived from a Lyapunov function, which plays a critical role in ensuring the stability and convergence of the training process. By leveraging the Lyapunov function, the proposed system guarantees that the training procedure does not interfere with or degrade the stability of the motor's rotational speed. This integration not only improves the robustness of the control system but also ensures that the motor operates with high efficiency and precision under varying and unpredictable external conditions.

This method thus offers a promising advancement in the field of motor control, particularly for systems operating in noisy or unstable environments.This paper is organized as follows: the second section is a place to declare the problem formulation. The main controller design is represented in the third section. The third section also gives the neural network technique for developing the disturbances estimator and the system stability analysis. The fourth section shows the effectiveness of contributions in a numerical simulation tool. The last section is the conclusion.

2. Problem Formulation

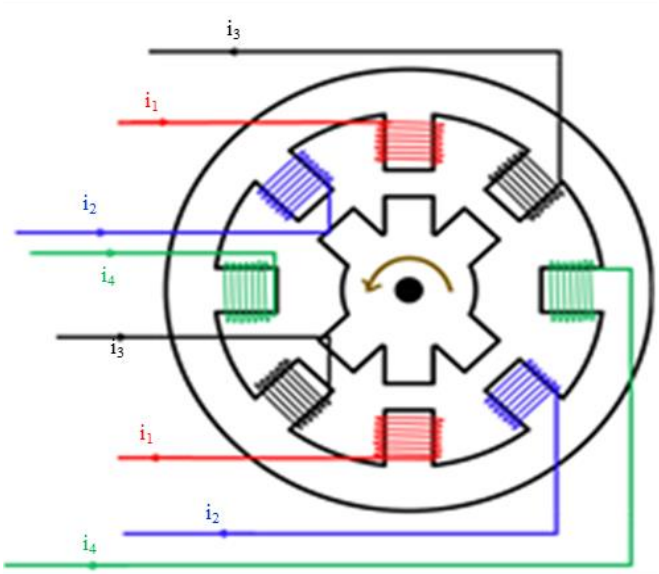

Fig. 1 The diagram in SRM's rotor and stator

The SRM system studied in this paper has 8 poles in the stator and 6 poles in the rotor, as shown in Figure 1. Therefore, the SRMs studied here are also known as SRMs 8/6. Additionally, the SRMs have four independent phases where the supply voltages for each phase are denoted as u_1, u_2, u_3 and u_4. The voltage supplied to each phase through the switching process is controlled by the operation of the Diode and IGBT. The current value in each phase is denoted by i_1, i_2, i_3 and i_4 respectively. The position of the SRMs' rotor is denoted by $\theta(t)$. The first derivative of $\theta(t)$is $\dot{\theta}(t) = \omega(t)$, which represents the rotation speed of the SRM system. Although there are four phases in an SRM system, only one phase is supplied with voltage at a given time. The voltage inputs u_1, i = 1, 2, 3, 4 are the input signals of the SRM system designed to make the rotation speed ω(t) stable at the desired value. The mathematical model of the system studied in [1] has the following form:

$$\begin{cases} x_1 = x_2 \\ x_2 = \sum_{i=1,2,3,4} f_i(x) + g_i(x)x_{i+2} + \delta \\ x_{i+2} = p_i(x) + q_i(x)k_i(t)u \end{cases} \quad (1)$$

Where the vector $x = (x_1 \;\; x_2 \ldots x_6)^T$, each element is $x_1 = \theta, x_2 = \omega,$ and $x_{3,4,5,6} = i_{1,2,3,4}$. These nonlinear dynamic functions $f_i(x), g_i(x), p_i(x)$ and $q_i(x)$ are calculated in [1]. δ symbolizes the external disturbances and unknown factors. u is the input voltage signal, and $\tau > 0$ is the time interval that the first phase is open. k_1 is a switch that can only accept two values, 0 when the first phase is closed or 1 when the first phase is opened. The time-varying graphs of k_1, k_2, k_3, k_4 are shown in Figure 2. Clearly, $k_i = k_1(t - (i - 1)\tau),\ i = 2, 3, 4$. The SRMs' model in Equation (1) can be expressed as a time-delay nonlinear system with $j = 3, 4, 5, 6$:

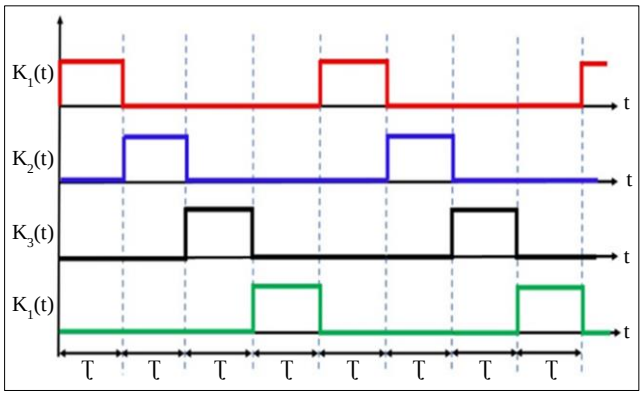

Fig. 2 The time-varying graph of $k_i(t), i = 1, 2, 3, 4$

$$\begin{cases} x_1 = x_2 \\ x_2 = \sum_{i=1,2,3,4} f_i(x) + g_i(x)x_{i+2} + \delta \\ x_{i+2} = p_i(x) + q_i(x)k_1(t - (j-3)\tau)u \end{cases} \quad (2)$$

Differentiating from both sides of x_2, the mathematical model of the rotational speed $x_2 = \omega(t)$ of the SRMs is rewritten as the following:

$$\begin{cases} \chi_1 = \chi_2 & (3) \\ \chi_3 = \left(\sum_{i=1,2,3,4} g_i(x)q_i(x)k_1(t - (j-3)\tau) \right) u + d & (4) \\ \chi_1 = \omega & (5) \end{cases}$$

Where d is a lumped function representing all the unknown external disturbances and nonlinear factors. Utilizing the notes $H\ (x, t - \tau) = \sum_{i=1,2,3,4} g_i(x)q_i(x)k_1(t - (j-3)\tau)$ is the lumped input gain function. Hence, the short presentation of the SRMs' model of rotational speed is:

$$\chi_1 = \chi_2 \quad (6)$$

$$\chi_2 = H\ (x, t - \tau)u + d \text{ n} \quad (7)$$

Remark 1. Although this system studied here is aspirated from the model proposed in [1], Rigatos et al. did not consider the undesired disturbances that existed during the SRMs' operation, as well as methods for compensating them. Thus, the research question here is more general than the research problem in [1].

Remark 2. Due to the instantaneous switching process of each phase, the SRM system provided here is considered a time-delay nonlinear system. The Dynamic Surface Control method proposed here is obviously more suitable for SRMs than the linearisation method proposed in [1].

Remark 3. According to [1], $H(x, t - \tau)u \neq 0$ for all $t \geq 0$. This condition ensures the controllability of the SRMs at all times.

3. Main Design

In this paper, the design procedure of the proposed DSC is presented step-by-step for easier readability.

3.1. Dynamic Surface Controller Design

Step 1 : Consider the first subsystem of the nonlinear and uncertain SRMs shown below:

$$\dot{\chi}_1 = \chi_2 \quad (8)$$

Denote $\omega_d = \omega_d(t)$ is the desired speed of the SRMs, and the tracking error $e = \omega_d - \omega = \omega_d - \chi_1$ is the error between the SRMs' speed and the reference value. The first-order derivation of *e* can be calculated as follows:

$$\dot{e} = \dot{\omega_d} - x_1 = \dot{\omega_d} - x_2 = \dot{\omega_d} - \alpha_1 - \varphi_1 \quad (9)$$

In (9), we denote $\chi_2 = \alpha_1 + \varphi_1$ where α_1 is considered the virtual control signal and $\varphi_1 = \chi_2 - \alpha_1$ is the error between χ_2 and α_1. To make $lim_{t\to+\infty} e(t) = 0$, using the candidate Lyapunov function $V_1 = \frac{\gamma_1}{2}e^2, \gamma_1 > 0$. Differentiating from both sides of the Lyapunov function V_1 given:

$$\dot{V_1} = \gamma_1 e\dot{e} = \gamma_1 e(\dot{\omega_d} - \alpha_1) - \gamma_1 e\varphi_1 \quad (10)$$

$$= \gamma_1 e(\dot{\omega_d} - \alpha_1 + c_1 e) - \gamma_1 e\varphi_1 - \gamma_1 c_1 e^2 \quad (11)$$

Therefore, if the virtual control input α_1 is chosen as:

$$\alpha_1 = \dot{\omega_d} + c_1 e \quad (12)$$

Obviously, α_1 is bounded. Then, the first-order derivation of the Lyapunov function V_1 becomes:

$$\dot{V_1} = -\gamma_1 c_1 e^2 - \gamma_1 e\varphi_1 \quad (13)$$

Obviously, if $\varphi_1 \to 0, \dot{V_1} \to -\gamma_1 c_1 e^2 < 0$ and $e \to 0$. Although it does not achieve $V_1 < 0$ in the first step because of the term $\gamma_1\varphi_1 e$, this term will be evaluated in the next step.

Step 2 : (Key step) The mission of this step is to steering $\varphi_1 = \chi_2 - \alpha_1 \to 0$. If $\varphi_1 \to 0, \chi_1 \to \omega_d$ according to the first step. To do this, consider the second subsystem of the nonlinear and uncertain SRMs shown below:

$$\dot{\chi_2} = H(x, t-\tau)u + d \quad (14)$$

Where d is the unknown factor. Using the second candidate, the Lyapunov function as follows:

$$V_2 = V_1 + \frac{\gamma_2}{2}\varphi_1^2 = \frac{\gamma_1}{2}e^2 + \frac{\gamma_2}{2}(x_2 - \alpha_1)^2 \quad (15)$$

Because, $\varphi_1 = \chi_2 - \alpha_1$ it can deduce that $\dot{\varphi_1} = \dot{\chi_2} - \dot{\alpha_1}$. Differentiating from both sides of Equation (15) and utilizing Equations (13), (14) yields:

$$\dot{V_2} = \begin{pmatrix} -\gamma_1 c_1 e^2 - \gamma_1 e\varphi_1 + \\ +\gamma_2\varphi_1(H(x,t)u + d - \dot{\alpha_1}) \end{pmatrix} \quad (16)$$

$$= \left(-\gamma_1 c_1 e^2 - \varphi_1 \begin{pmatrix} \gamma_2 H(x, t-\tau)u + \\ +\gamma_2 d - \gamma_2\alpha_1 - \gamma_2 e \end{pmatrix}\right) \quad (17)$$

To avoid the "explosion of terms" phenomenon when derivating the virtual control input α_1, this paper proposes using an LPF with a small time parameter to estimate the first-order derivation of α_1. The LPF used here is a linear-time-invariant (LTI) system whose state is denoted by z_1, input is α_1 and the mathematical model is expressed as:

$$T_f\dot{z_1} + z_1 = \alpha_1 \quad (18)$$

Because system (18) is LTI, whose input α_1 is bounded, it can be deduced that z_1 is also bounded. Therefore, if choosing the time parameter of the filter T_f to be small enough, the below estimation is held according to [19]:

$$\alpha_1 \approx z_1 \quad (19)$$

$$\Rightarrow \dot{\alpha_1} = \dot{z_1} = \frac{\alpha_1 - z_1}{T_f} + \epsilon = f(\alpha_1) + \epsilon \quad (20)$$

Where $\epsilon > 0$ is the estimation error of the utilized filter. From (16), V_1 becomes:

$$\dot{V_2} = \begin{bmatrix} -\gamma_1 c_1 e^2 + \varphi_1\gamma_2 H(x, t-\tau)u + \\ +\varphi_1\gamma_2 d - \varphi_1\gamma_2(f(\alpha_1) + \epsilon) - \\ -\varphi_1\gamma_1 e \end{bmatrix} \quad (21)$$

Due to the unknown factor *d* and ϵ, if the control signal *u* is designed as follows:

$$u = \frac{\gamma_2(f(\alpha_1) + \gamma_1 e - c_2\varphi_1 - b_1 s(\varphi_1) - \gamma_2\hat{d}}{\gamma_2 H(x, t-\tau)} \quad (22)$$

Where $\hat{d}$ is the estimation value of the unknown distance *d*. Noting that $\varphi_1 sign(\varphi_1) = sign^2(\varphi_1)|\varphi_1| = |\varphi_1|$ Then, the first-order derivative Lyapunov function V_2 becomes:

$$\dot{V_2} = -\gamma_1 c_1 e^2 - c_2\varphi_1^2 - b_1|\varphi_1| + \gamma_2\varphi_1\tilde{d} = \gamma_2\varphi_1\epsilon \quad (23)$$

$$\leq \gamma_1 c_1 e^2 - c_2\varphi_1^2 + \gamma_2\varphi_1\tilde{d} + (\gamma_2\epsilon - b_1)|\varphi_1| \quad (24)$$

$$\leq \gamma_1 c_1 e^2 - |\varphi_1|(c_2|\varphi_1|) - \gamma_2\tilde{d} + (\gamma_2\epsilon - b_1|\varphi_1|) \quad (25)$$

Where $d_m = sup_{t\geq 0} d(t) > 0$ is the upper boundary of the lumped disturbance $d, \tilde{d} = d - \hat{d}$ and $b_1, c_2 > 0$.

Hence, if parameter b_1 is chosen such that it satisfies $b_1 > \gamma_2\epsilon$, there always exists a positive real number λ such that:

$$V_2 \leq -\gamma_1 c_1 e^2 - |\varphi_1|\left(c_2|\varphi_1| - \gamma_2\left|\tilde{d}\right|\right) - \lambda|\varphi_1| \quad (26)$$

From (26), the error $\varphi_1 = \chi_2 - \alpha_1$ is always attracted in an invariant neighbourhood:

$$D = \left\{\varphi_1 \in \mathbb{R} \middle| |\varphi_1| < \frac{\gamma_2|\tilde{d}|}{c_2}\right\} \quad (27)$$

And for all $\varphi_1 \in D$, there always exists a number $\beta > 0$ such that $\dot{V_2}$ becomes:

$$\dot{V_2} \leq -\gamma_1 c_1 e^2 - (\beta + \lambda)|\varphi_1| < 0 \quad (28)$$

Therefore, it always has $lim_{t\to+\infty}\varphi_1(t) = c_2^{-1}\left|\tilde{d}\right|$ and $\chi_1 = \omega$ goes to the neighbourhood of the desired speed ω_d. The final task is to determine the updated law for $\hat{d}$ to make the minus $\left(\mathrm{d} - \hat{\mathrm{d}}\right)$ minimizing.

Remark 4. It can miniature the limitation $\lim_{t\to+\infty}\varphi_1(t) = c_2^{-1}\gamma_2|\tilde{d}|$ via selecting c_2 to be $c_2^{-1}\gamma_2|\tilde{d}| \to 0$ when $c_2 \to \infty$. However, the trade-off for this selection is the larger value of the control signal *u* shown in (22).

Remark 5. The condition $b_1 > \gamma_2\epsilon$ is sufficient for ensuring the stability of the closed-loop system. Nevertheless, due to the unknown filter's error ϵ, the easiest way to satisfy $b_1 > \gamma_2\epsilon$ is choosing the parameter b_1 to be larger enough. But similar to c_2, selecting a large value for b_1 can make the control signal u more "chattering".

Remark 6. Thank to the $\hat{d}$ term in the control signal *u* in (22), the miniature for the invariant set (27) is performed by only choosing large c_2. Otherwise, the condition (27) becomes $|\varphi_1| = c_2^{-1}\gamma_2|d|$ and adjusting for c_2 to be large has not yet been made $lim_{t\to+\infty}\varphi_1(t)$ to go to the small neighbourhood of the origin because of the limitation $|d|$ is maybe not bounded or small. If $\varphi_1(t)$ does not go to zero or a small enough neighbourhood of the origin, it can not make $\omega \to \omega_d$. That is a significance of the estimation term $\hat{d}$ for lumped disturbance added to the controller *u* in (22).

3.2. Disturbance Compensation

This section is the next step in designing the disturbance compensation-based DSC controller.

Step 3 : The architecture of the used neural network.

The Radial Basis Function (RBF) neural network is known as an effective tool for dealing with all uncertain factors and unknown disturbances that exist undesirably in a controlled closed-loop system. This reputation springs from the capacity to estimate unknown functions *f*(.) with an arbitrarily small error [17]. In the context of this paper, an RBF neural network is utilized to estimate the unknown term *d*. The utilized RBF network here includes 3 layers: input, output and hidden layer. There are N neurons in the hidden layer, and the ideal weight matrix of the network is characterized by $W \in \mathbb{R}^{Nx1}$ which satisfies $||W|| \le W_0$. The relationship between *d* and *W* is assumed as follows:

$$d = W^T\Phi(\chi_1, \chi_2) + \varepsilon \quad (29)$$

In (29), ε is the estimation error of the neural network satisfying $||\varepsilon|| \le \varepsilon^*$. The designed neural network has χ_1, χ_2 as the input and its output is the estimated value $\hat{d}(.)$ of *d*(.). It is calculated as the following [20]:

$$\hat{d} = \widehat{W}^T\Phi(\chi_1, \chi_2) \quad (30)$$

Where $\widehat{W}$ is the estimated weight. In (29) and (30), $\Phi(\chi_1, \chi_2) = col(\Phi_i(\chi_1, \chi_2)), i = 1,2,\dots,N$ symbolized the activation function, which is determined by:

$$\Phi(\chi_1, \chi_2) = \frac{exp\left(-\frac{\left\|\chi_1 - c_i\right\|^2}{b_i}\right) + exp\left(-\frac{\left\|\chi_2 - c_i\right\|^2}{b_i}\right)}{\sum_{j=1}^{N} exp\left(-\frac{\left\|\chi_1 - c_j\right\|^2}{b_j}\right) + exp\left(-\frac{\left\|\chi_2 - c_j\right\|^2}{b_j}\right)} \quad (31)$$

From (30) and (22), the disturbance compensation-based DSC through the neural network is expressed as follows:

$$\hat{u}_1 = \begin{bmatrix}\gamma_2 f(\alpha_1) + \gamma_1 e - c_2\varphi_1 - \\ -b_1 sign(\varphi_1) - \gamma_2\widehat{W}^T\Phi(\chi_1, \chi_2)\end{bmatrix} \quad (32)$$

$$\hat{u} = \frac{\hat{u}_1}{\gamma_2 H(x, t-\tau)} \quad (33)$$

Then, determining the updating law for minimizing $(d - \hat{d})$ means finding the online training rule for $\widehat{W}$ such that $\widehat{W} \to W$. This task is performed via a Lyapunov function defined in the final key step.

Remark 7. It would like to note that several neural network architectures have been developed recently [21]. Nevertheless, the main task in control engineering is stabilizing the system states, and the RBF utilized here with a simple structure and the less number of neurons in the hidden layer facilitates the application of the real world and saves computational memory.

Step 4 : (Key step) Designing the online training rule for the network's weight

To design the training rule for $\widehat{W}$, using the candidate Lyapunov function:

$$V_3 = V_2 + \frac{\gamma}{2}\widetilde{W}^T F^{-1}\widetilde{W} \quad (34)$$

Where $\gamma > 0, \widetilde{W} = W - \widehat{W}$ and $\dot{\widetilde{W}} = -\dot{\widehat{W}}$. Assuming that the controller's parameter b_1 is satisfied the condition $b_1 > \gamma_2\dot{o}$. Differentiating from both sides of (34) and using the Equation (26) yield:

$$\dot{V}_3 \le \dot{V}_2 + \gamma\dot{W}^T F^{-1}\widetilde{W} \quad (35)$$

$$\le \gamma_1 c_1 e^2 - \Phi_1(\varphi_1) + \gamma_2\varphi_1\tilde{d} + \gamma\widetilde{W}^T F^{-1}\dot{\widetilde{W}} \quad (36)$$

Where $\Phi_1(\varphi_1) = c_1\varphi_1^2 + \lambda|\varphi_1| > 0$ and noting that from Equations (29), (30):

$$\begin{aligned}\tilde{d} &= d - \hat{d} = \left(W - \widehat{W}\right)^T\phi(\chi_1, \chi_2) + \varepsilon \\ &= \widetilde{W}^T\phi(\chi_1, \chi_2) + \varepsilon\end{aligned} \quad (37)$$

Substituting Equation (37) into (36) gives:

$$\dot{V}_3 \le \begin{bmatrix}-\gamma_1 c_1 e^2 - \lambda|\varphi_1| - |\varphi_1|(c_2|\varphi_1| - \gamma_1\varepsilon^*) + \\ +\widetilde{W}^T\gamma_2\varphi_1\phi(\chi_1, \chi_2) - \gamma F^{-1}\dot{\widehat{W}}\end{bmatrix} \quad (38)$$

Therefore, from Equation (38), if the estimated weight $\hat{W}$ is updated as the following:

$$\dot{\widehat{W}} = \gamma^{-1}\gamma_2 F\phi(\chi_1, \chi_2)\varphi_1 \quad (39)$$

Then the error $\varphi_1 = \chi_2 - \alpha_1$ is always attracted in an invariant neighbourhood:

$$D^* = \{\varphi_1 \in \mathbb{R} | |\varphi_1| < c_2^{-1}\gamma_2\varepsilon^*\} \quad (40)$$

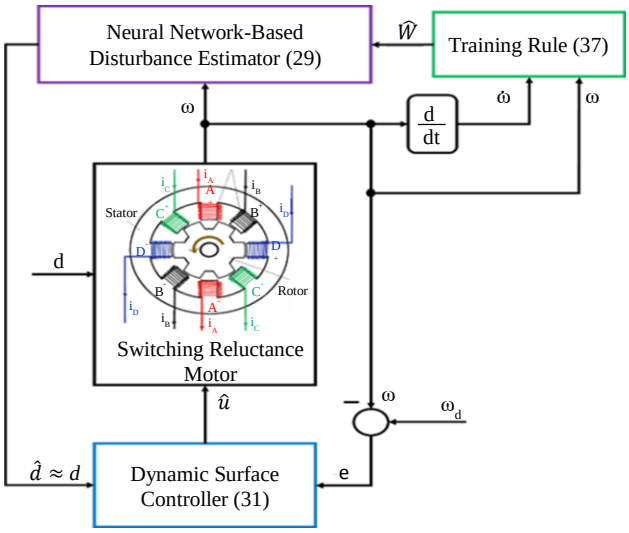

Fig. 3 The control scheme of the DSC controller with disturbance rejection

And the larger the parameter c_2 is, the smaller the neighbourhood D^* is. Finally, the cooperation control scheme between the DSC controller and the disturbance estimator is shown in Figure 3.

4. Numerical Simulation

The effectiveness of the proposed control strategy will be verified through simulation on Mat-lab/Simulink with two scenarios and compared with the traditional DSC method. The parameters of the SRMs are given in [1] and listed as:

$$J = 9.68\text{x}10^3(kg/m^2),\ B = 0.21,\ R = 0.05\ (\Omega)$$

$$l = 2(m), \alpha = 1.5\text{x}10^{-3}(H), b = 1.364\text{x}10^{-3}(H)$$

The parameters for the DSC controller are $c_1 = 1, c_2 = 3, \gamma_1 = \gamma_2 = \gamma_3 = \gamma = 1, N = 20,\ F = diag(40,41,\dots,59)$. The time parameter for LPF is chosen as $T_f = 0.025(s)$

Scenario 1 : Verify the disturbance rejection performance

Remark 6 emphasizes that the control performance is so much affected by the estimation results of lumped disturbance d.

Thus, it is necessary to verify the estimation result $\hat{d}$ before validating the rational speed's control process, the lumped disturbance d is assumed to be the bandwidth white noise and pulse noise whose amplitude is up to ± 100. The simulation result is shown in Figure 4 and Figure 5. As can be seen from Figures 4 and 5, the estimated disturbance $\hat{d}$ tracks to the real lumped disturbance d in a short interval. This convergence completely satisfies the Lyapunov function and online training rule for the RBF neural network presented in section 3.2. It needs to be emphasized that it is not necessary to make $\hat{d} = d$, that the proposed disturbance estimator made $\hat{d} \to d$ is enough to help out that the disturbance rejection-based DSC controller steered the SRMs' speed when the errors are small enough.

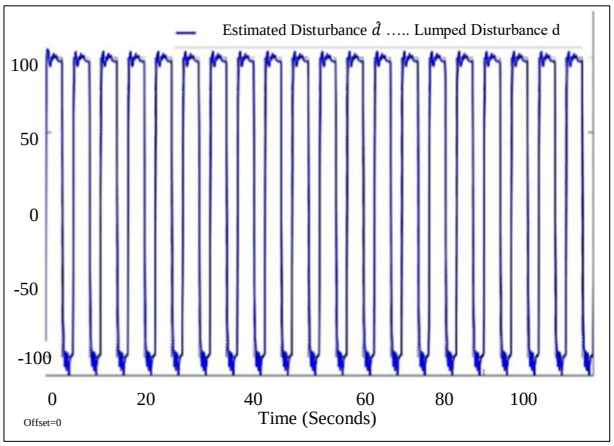

Fig. 4 Estimation disturbance performance with the pulse noise

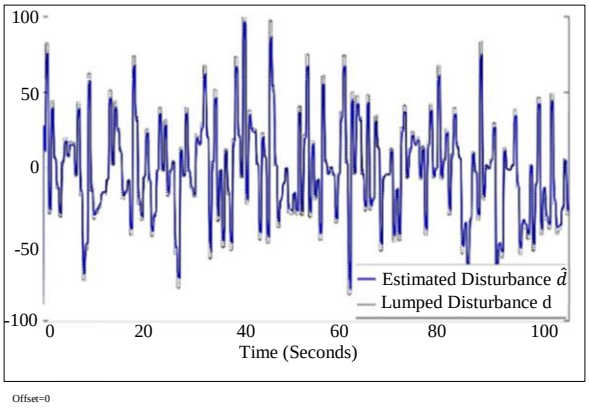

Fig. 5 Estimation disturbance performance with the white noise

This feature reaffirmed the effectiveness of the cooperation control scheme. Thanks to the disturbance compensation of the neural network, all the unknown and uncertain factors are rejected; thereby, the control performance is improved. It will be shown in the next scenario.

Scenario 2 : Verify the ability to stabilize the rotational speed at desired values

In this scenario, the desired speed for SRMs is defined as:

$$\omega_d = \begin{cases} 15[rad/s], if & t \le 20s \\ 10[rad/s], if & t > 20s \end{cases} \quad (40)$$

This scenario will compare the effectiveness of the proposed DSC controller in stabilizing SRMs' rotational speed to that of the DSC-only controller and Backstepping controller. The control signal for the DSC-only controller is studied in [7], and its formula is below:

$$u = \frac{\gamma_2 f(\alpha_1) + \gamma_1 e - c_2\varphi_1 - b_1 sign(\varphi_1)}{\gamma_2 H(x, t-\tau)} \quad (42)$$

And the Backstepping controller is given by:

$$u = \frac{\gamma_2 \dot{\alpha_1} + \gamma_1 e - c_2\varphi_1 - b_1 sign(\varphi_1)}{\gamma_2 H(x, t-\tau)} \quad (43)$$

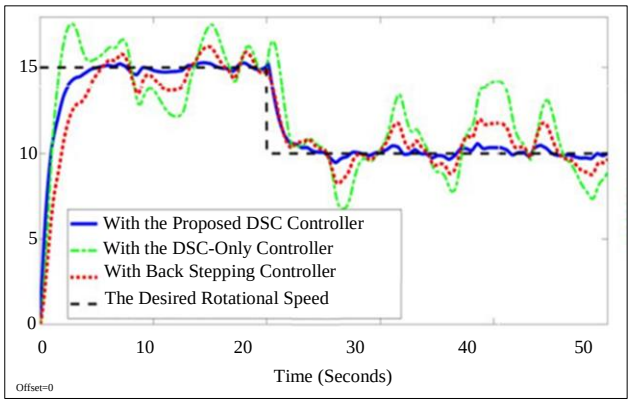

Fig. 6 Rotational Speed of the SRMs with different controllers

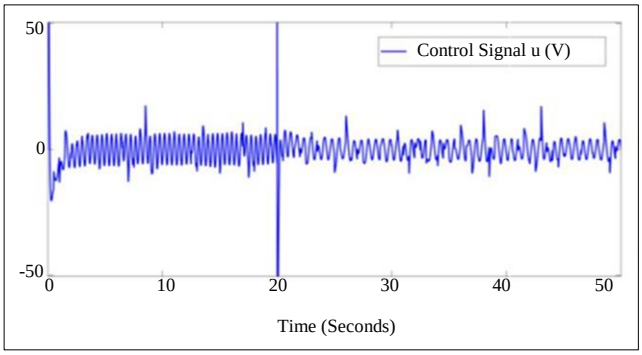

Fig. 7 Control signal of the proposed controller

Figure 6 clearly illustrates the performance in stabilizing the rotational speed at the desired value of three controllers. The proposed scheme's effectiveness, constructed from the DSC controller and neural network-based disturbance estimator, has better quality than the other two controllers. The maximum value of the tracking error of the proposed control scheme is only 2% around the reference compared to 15% on the Backstepping controller and 20% on the DSC-only controller. The reason for this lies in the term $\hat{d}$ in the controller. Thanks to the disturbance estimator, all the unknown and uncertain factors are annihilated from the closed-loop system. Thus, the control performance is enhanced. Compared to the robust control method H_∞ in [1], this proposed DSC controller can be performed without linearisation and maintain the rotational speed at the desired value regardless of large noises and external disturbances. Additionally, Figure 6 shows the control signal u of the studied SRMs. The voltage input is within the allowed limitation and varies significantly because of the sudden change in desired speed. ω_d. These results are suitable for the theories presented in the above sections.

5. Conclusion and Future Work

In this paper, the disturbance compensation-based DSC is applied to stabilize the rotational speech of SRMs at the desired value and reduce the influence of external disturbance in the control performance. Thanks to the low pass filter integrated into the control design procedure for estimation derivative, the undesired phenomenon called "explosion of terms" is eliminated. Therefore, the computational burden is reduced. Besides, All the external disturbances are combined into a unique lumped vector and rejected via an online training neural network, thereby lifting the control quality. The results are simulated on the Matlab-Simulink platform, and their effectiveness is compared with the simulation results using the backstepping technique and traditional DSC method. The achieved results emphasis that the control performance of the disturbance compensation-based DSC method under the influence of high-order noise is better than that of using traditional methods such as back stepping and DSC-only methods. The limitation of the proposed method that can be observed is the dependence on the control gain function $H(x, t-\tau)$, leading to mitigating the quality of speed stability in the event of this function being uncertain or changed randomly. Therefore, in the future, this method will focus on improving the adaption of the control scheme to address the undesired changes in the control gain function, where the RBF network is a continuous prospective candidate to apply because of its simple structure and training with ease.

Funding Statement

The research leading to these results has been sponsored by Hanoi University of Industry, Hanoi, Vietnam, under the project with Grant number 08/2024-RD/HĐ-ĐHCN.

Acknowledgements

The authors would like to thank colleagues at Hanoi University of Industry and Phenikaa University, Hanoi, Vietnam, for their constructive support and professional suggestions.

References

[1] Gerasimos Rigatos, Pierluigi Siano, and Sul Ademi, "Nonlinear H-Infinity Control For Switched Reluctance Machines," *Nonlinear Engineering*, vol. 9, no. 1, pp. 14-27, 2019. [CrossRef] [Google Scholar] [Publisher Link]

[2] JIn-Woo Ahn, *Switched Reluctance Motor*, Torque Control, pp. 201-252, 2011. [CrossRef] [Google Scholar] [Publisher Link]

[3] Ramu Krishnan, *Switched Reluctance Motor Drives: Modeling, Simulation, Analysis, Design, and Applications*, 1st ed., CRC Press, Boca Raton, 2017. [CrossRef] [Google Scholar] [Publisher Link]

[4] Jiajun Wang, "Speed-Assigned Position Tracking Control of SRM with Adaptive Backstepping Control," *IEEE/CAA Journal of Automatica Sinica*, vol. 5, no. 6, pp. 1128-1135, 2016. [CrossRef] [Google Scholar] [Publisher Link]

[5] Xiaodong Sun, "Optimal Design of Terminal Sliding Mode Controller for Direct Torque Control of SRMs," *IEEE Transactions on Transportation Electrification*, vol. 8, no. 1, pp. 1445-1453, 2021. [CrossRef] [Google Scholar] [Publisher Link]

[6] Muhammad Rafiq et al., "A Second Order Sliding Mode Control Design of a Switched Reluctance Motor using Super Twisting Algorithm," *Simulation Modelling Practice and Theory*, vol. 25, pp. 106-117, 2012. [CrossRef] [Google Scholar] [Publisher Link]

[7] Phi Hoang Nha et al., "Backstepping Control using Nonlinear State Observer for Switched Reluctance Motor," *Vietnam Journal of Science and Technology*, vol. 60, no. 3, pp. 554-568, 2022. [Google Scholar] [Publisher Link]

[8] Y. Boumaalif, and H. Ouadi, "A Nonlinear SRM Controller Design for Torque Ripple Reduction with Accounting for Magnetic Saturation," *IFAC-PapersOnLine*, vol. 55, no. 12, pp. 240-245, 2022. [CrossRef] [Google Scholar] [Publisher Link]

[9] Liyun Feng et al., "A Review on Control Techniques of Switched Reluctance Motors for Performance Improvement," *Renewable and Sustainable Energy Reviews*, vol. 199, 2024. [CrossRef] [Google Scholar] [Publisher Link]

[10] Ali Bouklata et al., "Advanced Control Strategy of Switched Reluctance Generator-Based Wind Energy Conversion Systems Using Backstepping and Extremum Seeking Techniques," *IFAC-PapersOnLine*, vol. 58, pp. 13, pp. 593-598, 2024. [CrossRef] [Google Scholar] [Publisher Link]

[11] Xiaodong Sun et al., "Position Sensorless Control of SRMs Based On Improved Sliding Mode Speed Controller and Position Observer," *IEEE Transactions on Industrial Electronics*, vol. 72, no. 1, pp. 100-110, 2025. [CrossRef] [Google Scholar] [Publisher Link]

[12] Jundi Sun et al., "Sliding Mode-Observer-Based Position Estimation For Sensorless Control of the Planar Switched Reluctance Motor," *IEEE Access*, vol. 7, pp. 61034-61045, 2019. [CrossRef] [Google Scholar] [Publisher Link]

[13] Phi Hoang Nha et al., "Backstepping Control using Nonlinear State Observer for Switched Reluctance Motor," *Vietnam Journal of Science and Technology*, vol. 60, no. 3, pp. 554-568, 2022. [Google Scholar] [Publisher Link]

[14] Arun Chithrabhanu, and Krishna Vasudevan, "Current Sharing Function Based Torque Ripple Reduction Strategy for Switched Reluctance Motor Drives," *In 2021 IEEE 12th Energy Conversion Congress & Exposition Asia (ECCE-Asia)*, Singapore, pp. 2381-2386, 2021. [CrossRef] [Google Scholar] [Publisher Link]

[15] Ali Abdel-Aziz, Mohamed Elgenedy, and Barry Williams, "Review of Switched Reluctance Motor Converters and Torque Ripple Minimization Techniques for Electric Vehicle Applications," *Energies*, vol. 17, no.13, pp. 1-26, 2024. [CrossRef] [Google Scholar] [Publisher Link]

[16] Hüseyin Çalik et al., "A Study on Torque Ripple Improvement Compared to a Modified Rotor and Stator Poles SRMs with Classical SRMs using Dynamic and FFT Analysis," *Electric Power Components and Systems*, vol. 51, no. 13, pp. 1328-1337, 2023. [CrossRef] [Google Scholar] [Publisher Link]

[17] Dingxin He, Haoping Wang, and Yang Tian. "Model Free Prescribed-Time Control Under Input Amplitude and Rate Saturations for Uncertain Mechatronic Systems with Mismatched Disturbances". *IEEE Transactions on Circuits and Systems II: Express Briefs*, vol. 71, no. 1 pp. 201-205, 2024. [CrossRef] [Google Scholar] [Publisher Link]

[18] Afshin Izadian, *Fundamentals of Modern Electric Circuit Analysis and Filter Synthesis*, A Transfer Function Approach, 2nd ed., Springer, 2019. [CrossRef] [Google Scholar] [Publisher Link]

[19] J.C. Das, *Power System Harmonics and Passive Filter Design*, IEEE Press and Wiley, 2015. [CrossRef] [Google Scholar] [Publisher Link]

[20] Haijiao Yang, and Dan Ye, "Adaptive Fixed-Time Bipartite Tracking Consensus Control for Unknown Nonlinear Multi-Agent Systems: An Information Classification Mechanism," *Information Sciences*, vol. 459, pp. 238-254, 2018. [CrossRef] [Google Scholar] [Publisher Link]

[21] Shuang Cong, and Yang Zhou, "A Review of Convolutional Neural Network Architectures and Their Optimizations," *Artificial Intelligence Review*, vol. 56, no. 3, pp. 1905-1969, 2023. [CrossRef] [Google Scholar] [Publisher Link]